Electronic Supplementary Material (ESI) for Physical Chemistry Chemical Physics

Supporting Information:

Unique Reactivity of Fe Nanoparticles-Defective Graphene Composites toward NH_x (x=0, 1, 2, 3) Adsorption: A First-principles Study

Xin Liu†‡, Changgong Meng†, Yu Han‡**

† School of Chemistry, Dalian University of Technology, Dalian, 116024, P. R. China

‡ Advanced Membrane and Porous Materials Center, King Abdullah University of Science and Technology, Thuwal, 23955-6900, Kingdom of Saudi Arabia

---

Corresponding Authors:

Dr. Xin Liu and Prof. Yu Han

Tel: +86-411-84708545(XL), +966-2-8082407(YH)

Email: xliu@dlut.edu.cn(XL), yu.han@kaust.edu.sa (YH)

Computational Setups

The electronic structure of pristine graphene (PG), defective graphene substrates and Fe nanoparticle-graphene composites were explored within a c(4×8) supercell (an orthorhombic supercell of 19.73 × 17.09 × 16.00 $Å^3$) with respect to the two-atom unit cell of graphene. The vacancy sites were put at the center of the single vacancy graphene (SVG) and the B-doped and N-doped single vacancy graphene (BVG and NVG). The integration of the Brillouin zone was conducted with a 2 × 2 × 1 Monkhorst–Pack grid centered at the Γ-point.[1] The geometry optimization of the defective graphene was carried out using the same conditions as for the nanoparticle-graphene composites.

The bulk lattice parameter of Fe in the body-centered cubic structure was determined to be a=2.83Å, comparable with the experimental values (a=2.86 Å) and theoretical results (a=2.83 Å).[2,3] Based on this, the geometry of the Fe_{13} particle was further optimized in a 25.10× 25.20× 25.30 $Å^3$ orthorhombic cell. The Brillouin zone integration was carried out only for the Γ-point. Among sub-nanometer-sized Fe_n particles, 13 is a magic number and the groundstate Fe_{13} icosahedral is highly stable and able to survive even in interactions with graphene substrate. It is thus suitable to illustrate the impact of the interaction between Fe nanoparticles and graphene substrates on catalytic performance.[4,5] The calculated Fe_{13} particle had icosahedral symmetry with a total spin of 44.00 μ_B.[4]

Construction of Models for Fe_{13}-Graphene Composites

An Fe_{13} nanoparticle with icosahedral symmetry has equilavent surface atoms, edges, and surfaces. Therefore, the possible interaction modes between graphene and the particle can be defined by the groups of atoms involved in the formation of the interfacial interaction. Several interaction modes were selected as the initial structure for the structure optimization (See Figure S1 for detail), including the atop-atop mode (A) where the Fe particle interacts with the graphene through only 1 Fe-C bond; the edge-hole mode (B) where 1 edge of the Fe particle interacts with 2 adjacent C_6 rings; the edge-counter bridge mode (C) where 1 edge of the Fe particle interacts with 2 counter bridge sites of 1 C_6 ring of the graphene; the surface-hole mode (D) where 1 surface of the icosahedral interacts with 3 nearest neighboring C_6 rings; and the surface-atop mode (E) where 1 surface of the Fe particle interacts with 3 C atoms connected to the same C atom. Six additional modes are also considered for a Fe particle deposited on PG: the surface-bridge mode (F) where 1 surface of the Fe particle interacts with 3 C=C bonds of the 1 C_6 ring; the atop-hole mode (G) where 1 atom of the Fe particle interacts with 6 C atoms of the same C_6 ring; the surface-atop mode (H) where 1 surface of the Fe_{13} icosahedral acts as the interface by interacting with 3 C atoms of the same C_6 ring on the graphene; the atop-bridge mode (I) where 1 atom of the Fe particle interacts with 1 C=C bond of a C_6 ring; the edge-counter atoms mode (J) where 1 edge of the Fe particle interacts with 2 diagonal C atoms of the same C_6 ring; and the edge-bridge mode (K) where 1 edge of the Fe particle interacts with 1 C=C bond of a C_6 ring.

Instead of presenting a large gap at the Γ-point on PG, there are unpaired sp^2 dangling bonds localized around the vacant site on SVG. The existence of these dangling bonds contributes to the DOS intensity around E_F and results in the high reactivity of the SVG.[6-8] This high reactivity of the SVG will inevitably give rise to the E_b. The calculated E_b of a single Fe atom at the vacant site was -6.98 eV, and the E_b of a Fe atom on PG was only -1.45 eV at the most preferable 6-fold hollow site. Therefore, when a vacant site is generated around PG-F, PG-G, PG-H, PG-I, PG-J and PG-K, the binding between the Fe_{13} particle and the single

vacancy site is high enough for the particle to rotate and move to the single vacancy and deform to other modes, and these modes were not included when studying the Fe-defective graphene composites.

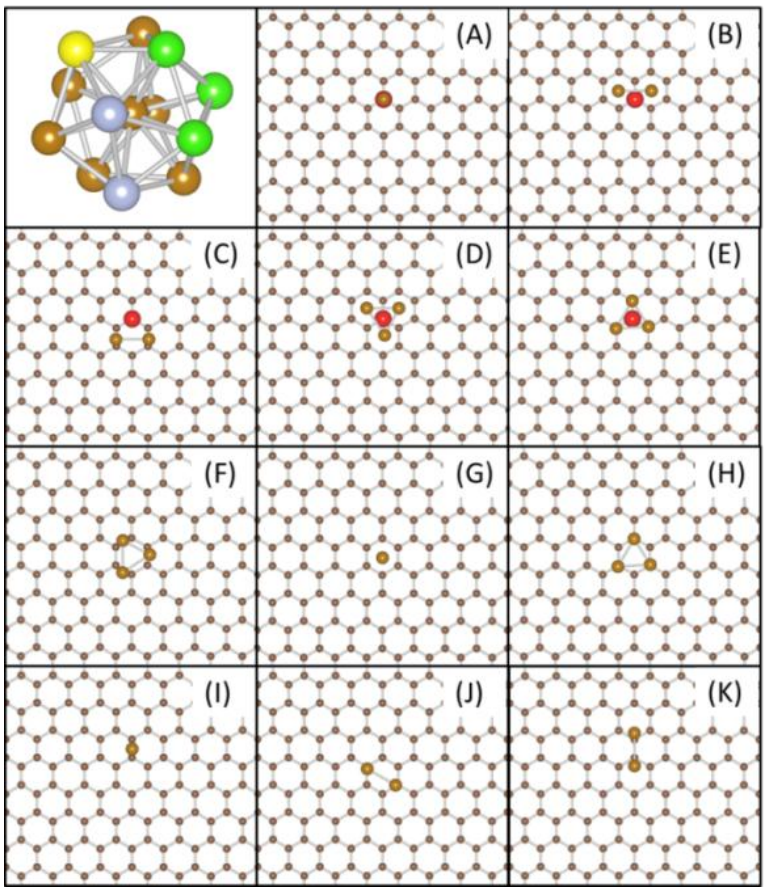

Figure S1 Structures of the interaction modes constructed for Fe_{13}-PG and Fe_{13}-SVG composites. (C: red and brown; Fe: dark yellow, green, yellow and blue). The red C atoms indicate the vacant sites of SVG. The green Fe atoms construct a surface, the blue Fe atoms constitute an edge, and the yellow atom indicates an atom of the Fe_{13} nanoparticle as the interface for deposition on PG and SVG. For clarity, only the interfacial Fe atoms are presented. See the text for the definitions of (A-K).

Electronic structure of Fe_{13}-PG composites

The optimized structures, adsorption energies and magnetic momentums for Fe_{13} nanoparticle deposition on PG are summarized in Table S1. Among the optimized modes of Fe_{13}-PG composites, the PG-F mode, where the Fe_{13} particle is slightly deformed to bind the graphene with 3 Fe atoms to 3 C=C bonds of 1 C_6 ring, is favored energetically (Figure S2b). The E_b of the PG-F mode is -0.87 eV, and the E_b of all the other interaction modes considered are less than -0.87 eV. These results compare well with the E_b values of Fe atoms or dimers on PG reported by Johll *et al*.[9] It should be noted that the calculated E_b of Fe_{13} particles on graphene is lower than that of a single Fe atom or a Fe dimer. This is due to fact that the Fe_{13} icosahedral is highly stable as compared with a single Fe atom or a Fe dimer.[4,5] The small E_b can be attributed to the surface energy of PG, and the negative values indicate that the deposition is thermodynamically favored. The DOS analysis (Figure S2a) shows that the states around the E_F are contributed mainly by the *d*-states of Fe, making atoms in the particle highly reactive. The DOS of the Fe states overlaps with the C states in the energy range [-7.0 eV, E_F], showing that the nature of the interaction is between Fe-*dsp* states and C-*sp* states.

Table S1. Optimized structures, magnetic momentums and adsorption energies for Fe_{13}-PG composites.

Model	E_b (eV)	μ^a (μ_B)	Min Fe-C (Å)[b]	Min/Max Fe-Fe (Å)[c]
PG-A	-0.02	34	2.20	2.34/2.61
PG-B	-0.17	34	2.18	2.31/2.67
PG-C	-0.24	34	2.13	2.29/2.73
PG-D	-0.70	38	2.18	2.29/2.80
PG-E	-0.69	38	2.14	2.31/2.73
PG-F	-0.87	38	2.15	2.32/2.72
PG-G	-0.06	34	2.19	2.34/2.56
PG-H	-0.48	37	2.10	2.28/2.71
PG-I	-0.04	34	2.20	2.33/2.63
PG-J	-0.16	35	2.18	2.31/2.69
PG-K	-0.24	34	2.12	2.29/2.64

[a] Magnetic momentum of the composites. The magnetic momentum for freestanding Fe_{13} particle is 44 μ_B.
[b] The minimum Fe-C distance at the Fe nanoparticle-PG interface.
[c] The minimum and maximum Fe-Fe distance inside the Fe nanoparticle. The maximum Fe-Fe distance is 2.55 Å, and the minimum Fe-Fe distance is 2.33 Å for the freestanding Fe_{13} particle.

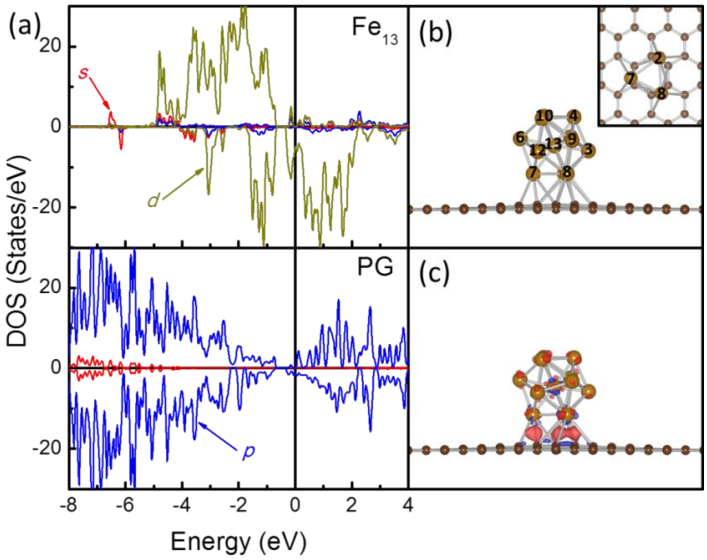

Figure S2. The DOS of interfacial C and Fe atoms for PG-F (a), optimized structure (b), and contour plot of the differential charge density of PG-F. The inset in (b) shows the position of interfacial Fe atoms with Fe-C distances less than 3.0 Å. (Brown: C; Dark yellow: Fe; the charge accumulation region is rendered in red, the charge depletion region is in blue, and the isovalue is ±0.005 a.u.)

References:

(1) Monkhorst, H. J.; Pack, J. D. *Phys. Rev. B* **1976**, *13*, 5188.
(2) Kohlhaas, R.; Duenner, P. *Z. Angew. Phys.* **1967**, *24*, 245.
(3) Blonski, P.; Kiejna, A. *Vacuum* **2004**, *74*, 179.
(4) Rollmann, G.; Entel, P.; Sahoo, S. *Comput. Mater. Sci.* **2006**, *35*, 275.
(5) Postnikov, A. V.; Entel, P.; Soler, J. M. *Eur. Phys. J. D* **2003**, *25*, 261.
(6) Liu, X.; Li, L.; Meng, C. G.; Han, Y. *J. Phys. Chem. C* **2012**, *116*, 2710.
(7) Liu, X.; Meng, C. G.; Han, Y. *Nanoscale* **2012**, *4*, 2288.
(8) Liu, X.; Zhang, S. B.; Ma, X. C.; Jia, J. F.; Xue, Q. K.; Bao, X. H.; Li, W. X. *Appl. Phys. Lett.* **2008**, *93*, 093105.
(9) Johll, H.; Kang, H. C.; Tok, E. S. *Phys. Rev. B* **2009**, *79*, 245416.